https://doi.org/10.33261/jaaru.2020.27.1.004 *Association of Arab Universities Journal of Engineering Sciences (2020) 27(1): 30–43*

Association of Arab Universities Journal of Engineering Sciences

مجلة اتحاد الجامعات العربية للدراسات والبحوث الهندسية

Comparison Between Commercial and Synthesized Fe_3O_4 Nanoparticles for Removal of Heavy Metal Contaminants in Wastewater

Farouk Abdullah Rasheed Alkurdy[1], and Shahlaa Esmail Ebrahim[2,*]

[1] *Civil Engineering, University of Sulaimani, Sulaimani, Iraq, frouk.rasheed@univsul.edu.iq.*

[2] *Environmental engineering Department, University of Baghdad, Baghdad, Iraq, shahlaa.ebrahim@fulbrightmail.org*

**Corresponding author: Farouk Abdullah Rasheed Alkurdy, frouk.rasheed@univsul.edu.iq.*

Published online: 31 March 2020

Abstract— Wastewater polluted with harmful heavy metal presently becomes a crucial environmental issue throughout the world. In this study, commercial and synthesized Fe_3O_4 nanoparticles were functioned to remove lead, nickel and cadmium ions in single element system. Experimental conditions including pH, contact time and metal ion concentrations were tested. The isothermal equilibrium for single component system was favorable and the maximum uptake of lead, nickel and cadmium ions adsorbed on commercial Fe_3O_4 were 35.3, 5.18 and 18.16 mg/g respectively while 31.5, 4.36 and 20.56 mg/g on synthesized one at optimum pH 6 for an hour of equilibrium contact time. The isotherm data resulted from both adsorbents fitted well with Freundlich model. The experiments demonstrates that the performance of synthesized nanosorbent which is economically convenient to be used, approaches the effectiveness of commercial Fe_3O_4. Therefore, prepared nanosorbent form was taken as practical adsorbent and utilized in binary and ternary systems to show the competition of metal contaminants. Results indicated that lead ions had rapid affinity to be sorbed on the nanoparticles while nickel solute had slow attraction. XRF X-ray fluorescence, TEM Transmission electron microscope, FTIR Fourier transfer infrared and XRD X-ray diffraction were also carried out to identify and demonstrate the properties of both nanosorbents.

Keywords— metal ion, nanosorbent, adsorption, wastewater

1. Introduction

Rapid expansion of industry and continual growth of human being populations create unhealthier environmental contamination than in the past. Increasing heavy metal pollutions resulted from modern industrialization and rapid urbanization is considered as a major issue in the environmental ecosystems [1]. Some heavy metals, unlike organic solutes, at low concentrations are crucial for many physiological and biochemical processes. However, at high concentrations, they cause hazards to human health and environment [6,18]. The metals which are extremely worried about are cadmium, mercury, lead, manganese, chromium, cobalt, copper, nickel, and zinc [9,10]. Although these metal elements are essential and useful technologically, their release through various industrial wastewater into environment and water sources cause serious public concerns due to non-biodegradability and their toxicity at relatively low concentrations [5,13,8]. These toxic metal ions are observed in effluent discharge of some industries like chemical production, leather, textiles, the plastic industry, storage batteries, mining, melting, metallurgical processes [1,35]. Those metals tend to store in organs of aquatic organisms and transfer to consumers, leading to various health problems [19]. Thus, heavy metals can accumulate in food chain through ecological prevailing and may present increasing long-term toxic effects [15,32].

The instantaneous removal of these toxic pollutants from wastewater is a noticeable issue in the aerobic and aquatic world. A number of physical and chemical methodologies have been developed to control these toxic contaminants successfully such as chemical precipitation technique, ion exchange practice, membrane separation processing and

electrochemical treatment [41,43]. All the above methods are costly, high energy input, large quantities of chemical reagents required, having high chemical sludge production and inefficient for low-level metal contamination removal from wastewater [4]. Therefore, cost effective alternative technologies for treatment of metal contaminated waste streams are needed. Adsorption is a common, effective, economical and satisfactory technique that widely used in elimination of toxic metal ions because of ease of operation, economic feasibility, wide availability and simplicity of design [8,23]. Furthermore, environmentally friendly adsorbent and applicable nanoparticles are widely familiar in research due to desirable and unique physical and chemical properties [34]. Nanoparticles exhibit good adsorption efficiency in water purification systems due to large surface area, high surface reactivity, simplicity in usage, great active sites for interaction with metallic species, strong adsorption ability, ease synthesis and no secondary pollutants [14,27]. Currently, nanosized metal oxides, including nanosized ferric oxides, manganese oxides, aluminum oxides, titanium oxides, magnesium oxides and cerium oxides, are classified as promising adsorbents for heavy metal removal from aqueous systems. Metal oxide nanosorbents should obey certain conditions: nontoxicity, high ability of adsorption, great potential of selectivity to different concentrations of pollutants and easily regeneration [38]. Recently, commercial and natural iron oxides have attracted attention most researchers because of their Nano-adsorptive properties [29]. In spite of being their ubiquitous availability in nature, iron oxides are the most popular nanoparticles having nanoscale zero-valent iron. Moreover, they possess different physicochemical properties due to the difference in their iron oxidation states leading to different capability for pollutant removal.

Velez et al. [36] confirmed that iron oxide nanoparticles have the capability to remove 70% of persistent mercury pollutant in wastewater and showed that the applied iron oxides nanoparticles have a narrow size distribution up to (~100nm). Mahdavi et al. [21] also investigated toxic heavy metal removal from wastewater using iron metal oxide nanoparticle adsorbent, which are completely different from other conventional adsorbent solids and the maximum uptake values of four elements (cadmium, lead, nickel and copper) together in multiple component solutions were 73 mg/g, In this investigation study, systematic laboratory examination of batch process was employed to explore the viability and effectiveness of commercial and synthesized iron oxide nanoparticles to remove lead, nickel and cadmium ions in single, binary, and ternary systems. This work also reports the preparation of nanoparticles in laboratory. and identification of the essential characterization of both nanosorbents through using (XRF, SEM, FTIR and XRD) techniques.

2. Materials and Methods

2.1 *Metal Solute Solutions*

Chemical reagent powders of Pb $(NO_3)_2$, Ni $(NO_3)_2.6H_2O$ and Cd $(NO_3)_2$ (BDH /England-purity 99.5 %) were used to prepare (1000 mg/l) a stock metal solution for each of lead, nickel and cadmium ions. Quantities of 1.6, 4.953 and 2.104 g of lead nitrate, nickel nitrate and cadmium nitrate respectively were weighed and mixed with 200 ml of deionized water and a volume of 10 ml of concentrated nitric acid. Once a uniform adsorbate solution was reached, Dilution was applied by the further addition of deionized water up to 1000 ml [11]. The desired normality was obtained after diluting a limited volume of concentrated solution with deionized water. Dissolved metal concentrations in solution were measured using an inductive couple plasma optical emission spectrometer (ICPOES-Optima 2100 DV, PerkinElmer Inc., UK).

2.2 *Nano adsorbent*

Two types of iron oxide Fe_3O_4 nanoparticles were applied in this research. Commercial form nanoparticles (acquired from Houston nanoparticle research in USA, TX 77084) and synthesized form prepared in laboratory were used as Nano sorbents to eliminate metal pollutants Pb (II), Ni (II) and Cd (II) from water. The overall goal was to characterize, utilize and ascertain the performance of both sorts in removal of metal ions. The one which had higher efficiency and less cost effective in removal of metal pollutants, used in binary and ternary systems.

2.3 *Fe_3O_4 nanoparticle preparation in laboratory*

Iron oxide (Fe_3O_4) nanoparticles are widespread in nature, have the structure of an inverse spinel and they differ from most other iron oxides in that they contain both Fe (II) and Fe (III). Co-precipitation is the most widely used method for the synthesis of the nanoparticles of controlled sizes [31,40]. The amount of 5.4 g ferric chloride hexahydrate ($FeCl_3.6H_2O$) and 3.6 g of technical urea $(NH_2)_2CO$ (purity 99 %, total nitrogen content 46 %, Prilled urea, Shandong factory, China) were weighed and mixed in a thermo conical flask using 200 ml distilled water. A water bath was turned on and set on 90±3˚C to heat the mixture until the color of the solution turned from clear orange to kaki. The liquid mixture was left for a while to cool down and then a magnetic stirrer with a speed of 600 rpm was used to mix the solution with an additional 2 g of ferrous chloride tetrahydrate ($FeCl_2.4H_2O$) for 15 minutes. Some drops of NaOH solution with molarity (2 mol/l) were gradually added until the pH value of the solution rose to above 10. Thus, a greenish precipitate was observed and poured into a plastic can with 500 ml capacity. Distilled water was added to fill the can and then sealed to prevent air from entering. Finally, the plastic container was left at room temperature for 7 h. The precipitated black color was filtrated using Whatman filter paper No.42, followed by washing with 500 ml of distilled water initially and then 100 ml of acetone later. The residue precipitate on the filter paper was oven-dried at 50˚C for 7 h [12]. **Figure 1** illustrates the schematic diagram for the preparation of raw iron oxide nanoparticles in laboratory.

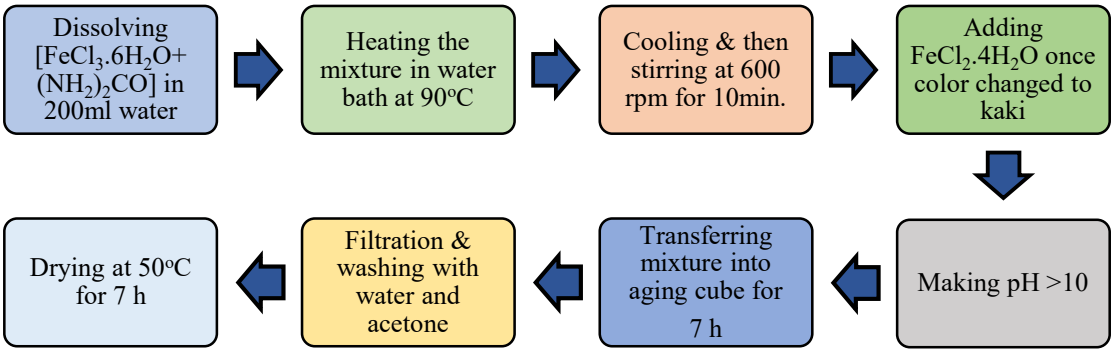

Figure1: Schematic diagram for the preparation of iron oxide nanoparticles in laboratory

The main physical properties of the commercial nanoparticles were procured from the purchased bottle label (Houston nanoparticle research in USA, TX 77084) while for synthesized one, various techniques in Kurdistan institution for strategic studies and scientific research were depended to measure its characteristics. **Table 1** shows the list of main physical features of both nanosorbents. Specific and external surface area characteristics of commercial nanosorbent were also evaluated and they are (63 and 61) m^2/g respectively while for synthesized type 58 and 55m^2/g respectively. The results showed that no substantial difference is existed between them. This demonstrates of having no essential porosity and upholding high surface area.

Table 1: The main physical properties of commercial and synthesized Fe_3O_4 nanoparticles

Physical properties	Commercial Fe_3O_4	Synthesized Fe_3O_4
Purity	98±%	97±%
Average Particle Size (nm)	20-30	50-80
External Surface Area(m^2/g)	61	55
Color Dark	Dark Brown	Clear brown
Morphology	Spherical	Spherical
Bulk Density (g/cm^3)	0.84	0.79
True Density (g/cm^3)	4.8-5.1	4.73

Both types of nanosorbents were also scanned under XRF technique (X-ray florescence, Spectro IQ11/Ametek, materials analysis division/Germany) to identify the main chemical composition involved in their structure. The results are illustrated in **Table 2** showing that Fe_2O_3 in both (commercial and synthesized) samples takes the largest quantity (72.74% and 54.85%) respectively. The higher percentage of Fe ions in the nanosorbent, the better attraction properties of the adsorbent sample to adsorb metal contaminants from bulk liquid will be. However, working on synthesized adsorbent is more economical compared to commercial one.

Table 2: Chemical composition of both Fe_3O_4 nanosorbent types by XRF

Compounds	Commercial Fe_3O_4	Synthesized Fe_3O_4
%Fe_2O_3	72.74	54.85
%SiO_2	0.112	0.113>
%Al_2O_3	0.178	0.203
%TiO_2	0.75	0.0064
%MnO	0.382	0.2
%MgO	1.268	0.26
%Cl	0.169	1.71
%CaO	0.197	0.011

3. Batch experiments

3.1 *Evaluation of optimum pH*

To find the optimum value of pH that gives maximum efficiency to remove metal ions, the following procedure was taken:

The amount of 0.5 g of commercial Fe_3O_4 nanoparticles was added separately to six volumetric flasks, each containing 100 ml of a single heavy metal solution with a concentration of 40 mg/l for Pb (II), Ni (II) and Cd (II) ions respectively. The pH value of the solutions in the six flasks was adjusted from 3-8 using 0.1 molar sodium hydroxide or nitric acid solution with an agitation speed of 200 rpm at a laboratory temperature of 20°C for an hour of contact time. Finally, separation of nanosorbent from metal solution was performed using U-shaped magnetic horseshoe part and samples of 10 ml from each volumetric flask were taken, filtered and measured in concentration by inductive couple plasma optical emission spectrophotometer (ICPOES). The same procedure was repeated for synthesized nanoparticle adsorbent.

3.2 *Equilibrium Contact Time*

Enough contact time is essential to establish the equilibrium time for maximum uptake. In the initial stage, the removal efficiency of metal ion is rapid due to availability of plenty effective active sites on the adsorbent surface. However, the process becomes slow in later periods. This means that the equilibrium status can be achieved [25]. The quantity of 0.5 g of each iron oxide nanosorbent separately was blended with 100 ml of single metal ion solutions in two flasks of 250ml capacity with a concentration of 40 mg/l for Pb(II), Ni(II), and Cd(II) ions. The solutions were adjusted to pH 6 and agitated with speed of 200rpm for different periods of time. Samples with a volume of 10ml at each period were taken at each period and their metal ion concentration measured using (ICPOES).

3.3 *Initial metal concentration influence*

Three distinctive concentrations of 15, 40 and 80 mg/l were utilized to show the effectiveness of solution strength on the functional efficiency of both nanosorbents towards the ultimate adsorption of metal ions. A mass of 0.5 g of each nanosorbent particles was mixed separately with 100 ml of single metal ion solution in a number of flasks of 250ml capacity with three distinctive concentrations of 15, 40 and 80 mg/l for each ion of Pb(II), Ni(II), and Cd(II). The solutions were adjusted to pH 6 with an agitation speed 200 rpm at 20°C. Samples with a volume of 10ml were taken at each period and their metal ion concentration measured using (ICPOES).

3.4 *Equilibrium isothermal investigation*

Different quantities of nanosorbent (0.05, 0.1, 0.2, 0.25, 0.3, 0.4, 0.6, 0.8, 1,1.2, and 1.4) g were used and put into 11 volumetric flasks of 250 ml. Solutions with the concentration of 40mg/l were prepared for single systems of lead, nickel and cadmium ions respectively and 100 ml from each solution was added to each flask. The pH value of solutions in the flasks was adjusted to desirable value of 6 using 0.1M sodium hydroxide or nitric acid. Thermoshaker was used to agitate continuously for an hour with a speed of 200 rpm and temperature 20°C. Nanosorbents from each flask were separated using a small magnetic horseshoe and the samples filtered through Whatman filter paper (No.1). Volume of 10 ml from each sample was taken and few droplets of the nitric acid added to lower its pH value below 2 to in order to fix the concentration of the heavy metals during storage of metal ions in the samples prior to analysis [25]. The final equilibrium concentrations were measured by (ICPOES). The uptake q_e and efficiency η of adsorbed metal ion is then calculated using the following formulas [22]:

$$q_e = \frac{V_l(C_o - C_e)}{W} \quad (1)$$

$$\eta\ \% = \frac{(C_o - C_e)}{C_o} \quad (2)$$

Where; C_o and C_e are initial and equilibrium metal concentration in the experiment solution respectively and V_l is metal solution volume in the flasks and W is the dosage of nanosorbents. Isothermal adsorption curves for each metal ions on both of nanosorbents were plotted based on the amount of adsorbed solute for each unit of weighted nanosorbent (q_e) versus the final equilibrium concentration of metal ions in the solution (C_e). The obtained experimental laboratory data from isothermal adsorption experiments was interrelated to two common non-linear adsorption model equations (Langmuir and Freundlich) through using of statistical software-version.8 to compute fundamental parameters of each model [37]. These models describe the energy distribution of active sites that can be homogeneous or heterogeneous. In addition, they suggested monolayer or multilayer adsorption and interactions between adsorbed molecules [33].

3.5 *The influence of multicomponent metals on nanosorption*

Mixed ion systems are normally existed in effluent discharge of various industries. In this system, only the greater and more efficient nanosorbent was utilized to eliminate metal contaminant ions in aqueous solution. The gained data for binary and ternary element systems were associated with two common models (Extended

Langmuir represented by equation (3) and Interaction Factor denoted by equation (4).

$$q_i = \frac{b_i q_{m,i} C_{e,i}}{\left(1 + \sum_{j=1}^{n} b_j C_{e,j}\right)} \quad (3)$$

$$q_i = \frac{b_i q_{m,i} \left(C_{e,i}/\eta_i\right)}{1 + \sum_{j=1}^{n} b_j \left(C_{e,j}/\eta_j\right)} \quad (4)$$

Interaction Factor (η_i)

$$= \frac{100}{N - P} \sum_{i=1}^{n} \left[\frac{\left(q_{exp} - q_{cal}\right)^2}{q_{exp}}\right] \quad (5)$$

Where bi and qm, are the Langmuir isotherm model parameters, $C_{e,i}$ is equilibrium concentration of metal ions. (N) and (P) are number of experimental data and interaction factor model parameter respectively. Statistical software-version,8 was again used to evaluate parameters of each model based on non-linear fit of the model equations to the experimental data.

3.6 *TEM scanning examination*

TEM scan has its strong points of interest as it appropriates direct pictures and local information on morphology, distribution and stage present of particles. The micrographs in Figure 1 provide information about size, shape and distribution of particles for both of biosorbent and synthesized Fe3O4 nanoparticles. The biosorbent exhibited a rough surface providing a large vacant area for metal ion interaction [40]. The images also demonstrate that small pores are existed on the biosorbent surface whereas no pore sizes are noticeable in the nanosorbent images. The existence of pore sizes on the surface of biosorbent is helpful for further uptake of solute pollutants from the bulk solution and enhance deeply intraparticle diffusion [40].

The size, shape and morphology surface of both samples of Fe_3O_4 nanoparticles were identified through TEM scanner. [42]. The images of both samples were analyzed through detection of electron reflection from the samples under 25.00KV.

3.7 *Fourier Transform Infrared analysis*

The presence of negative functional group charges on the raw iron oxide surface creates an affinity for electrical attraction of positive metal ions in bulk water liquid. Identification the type of efficient groups (carbonyl, carboxylic, hydroxyl and others) on external surface of nanosorbent requires Fourier Transfer Infrared investigation. One-gram mass of iron oxide nanosorbent from each type was taken and left in an oven set at 50°C for 24h, then analyzed by FTIR device (Shimadzu FTIR 8000 series spectrophotometer). FTIR technique was performed on both samples (commercial and synthesized Fe_3O_4 in laboratory.) in wave range of 4000–400cm^{-1} with a resolution of 4cm^{-1}.

XRD (X-ray diffraction) examination

Both commercial and synthesized nanoparticles were examined under XRD technique using (Xpert pro MPD- analytical, Holland) to reveal peaks associated to various compounds present in both nanosorbents.

4. Results and Discussion

4.1 *The influence of pH value*

Figure 2 demonstrates that the nanosorption efficiency of both sorbents was improved significantly with the increase in pH value due to deprotonation of nanosorbent surfaces making them behave as negatively charged which started attracting the positively charged metal ions. However, as pH value of solution is dropped, the charges of the surface will become totally positive, which will constrain approach of positively charged metal cations [30]. Both nanosorbents achieved maximum removal at pH 6.0 and then fell down. This because beyond the value of pH 6.0, precipitation will occur to heavy metals due to insoluble metal hydroxides, start precipitating in the solutions and make the true sorption studies impossible. This should be avoided during sorption experiments otherwise distinguish between sorption and precipitation of metals becomes hard [17] Therefore, pH 6.0 was used in all subsequent experiments. **Figure 2** also revealed that lead ions has the highest tendency to be adsorbed on both adsorbents while nickel has the least affinity to do so. These results are in compliance with what some investigators obtained [3,26]. Even though imported commercial Fe_3O_4 type is slightly more operative to remove lead and nickel, it is more reasonable and feasible to concern synthesized nanosorbent due to its cheapness and simplicity of preparation in laboratory. This can reduce importation of large amount of nanosorbents from abroad.

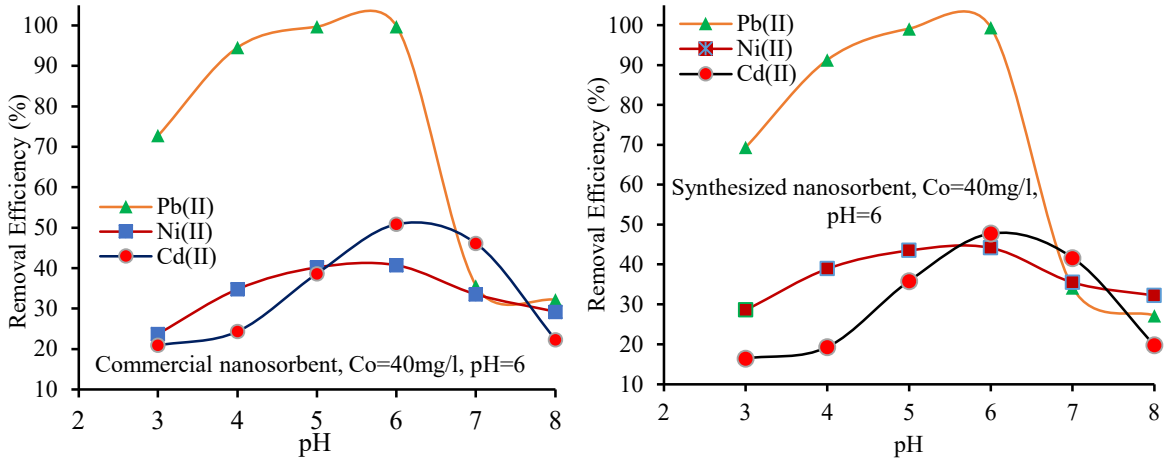

Figure 2: Effect of different pH on lead, nickel and cadmium uptake by Fe_3O_4 nanoparticles a) Commercial b) Synthesized.

4.2 *The effect of equilibrium contact time*

It was observed from **Figures 3** that the uptake of the three metal pollutants by both types of nanosorbents increased with having more contact time. No significant increase in the sorption was found after 20 min, and the adsorption was rapid. Metal concentration decreased rapidly during the first 20minutes and remain nearly constant after an hour of adsorption, suggesting that the adsorption is fast and reaches saturation within an hour. The reason is attributed to the fact that both iron oxide nanosorbents are a nonporous solid adsorbent, as verified by surface area and porosity measurement, where only adsorption occurs externally. This type of mass transfer adsorption needs less time to achieve equilibrium. This result is promising as equilibrium time, plays a major role in wastewater treatment plant in which economically viable [3]. These results agreed with what attained by Ebrahim et al. [10].

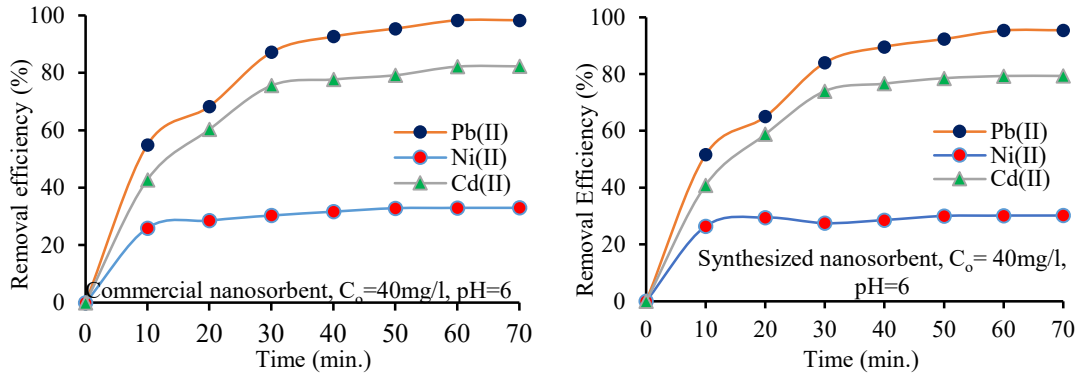

Figure 3: Equilibrium contact time for metal ions using Fe_3O_4 nanoparticles a) Commercial b) Synthesized.

4.3 *The influence of concentration strength*

Figure 4 illustrates that the ability of nanosorbents to remove metal ions was not changed drastically if intensity of concentration enhances from 15 to 40 mg/l. The reason is that one gram of nanosorbent has enough occupant sites for this extent of concentration. However, when concentrations trend up to 80 mg/l, no

adequate vacant places will be available to stick and collect these intensive concentrations [39]. Therefore, the fraction of nanosorption efficiency to remove metal ions was decreased but the uptake of metals on the nanosorbents increased due to high driving force between nanosorbent and solute ions [7]. These results corresponded with the outcomes gained by Vijayaraghavan and Yun [37].

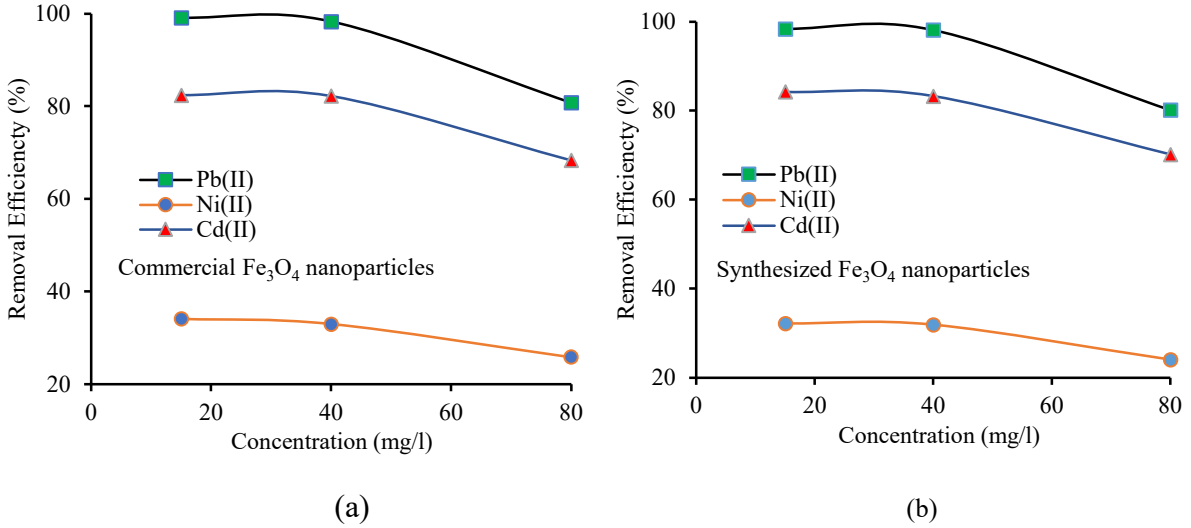

Figure 4: Removal efficiency percentage of Fe_3O_4 nanoparticles at various concentration, 20°C, pH=6 and contact time=60min. for a) Commercial b) Synthesized.

4.4 *Single component module*

Figure 5 shows single metal uptake system by both nanosorbents in solutions with concentration of 40 mg/l, pH value of 6 and dosage of 1.4 g/100 ml at 20°C. The maximum adsorption uptake of lead, nickel and cadmium respectively onto commercial adsorbent was 35.3, 5.18, 18.16 mg/g while the uptake onto synthesized adsorbent was 31.5, 4.36 and 20.56 mg/g. The maximum metal removal efficiency achieved with commercial nanosorbent was 100 %, 66.68 %, 96.38 % for lead, nickel and cadmium respectively. However, in state of using synthesized nanosorbent, the performance decreased slightly to 99.7 %, 65.5 % and 96.85 % respectively. The resulted data for single element system were interrelated with the isothermal models (Langmuir and Freundlich) as shown in **Table 3** using non-linear model equations corresponded well to experimental data. Both equations 6 and 7 represent Langmuir and Freundlich models respectively:

$$q_e = \frac{q_m\, b\, C_e}{(1+b\, C_e)} \qquad (6)$$

$$q_e = K C_e^{1/n} \qquad (7)$$

Where q_e denots the equilibrium metal uptake in (mg/g), q_m is the maximum ion uptake acheived on the nanosorbent in (mg/g), b is related to the extent affinity between the ions and nanosorbents in (l/mg). K corresponds to the maximum binding capacity; n, characterizes the affinity between the ions and nanosorbents; and C_e, is the equilibrium concentration in (mg/l).

Freundlich isotherm models was best fitted to the experimental data for Pb (II), Ni (II) and Cd (II) ions adsorption onto both types of iron oxide nanoparticles. It could also be illustrated from **Figure 5** that advanced adsorption removal for lead was achieved at low dose of Fe_3O_4 nanoparticles and its more rapid affinity towards the nanoparticles opposed to other metal ions revealing presence of various electrical attraction between cation lead metal and negative adsorption functional sites. Additionally, Lead ion possesses the smallest hydration radius while nickel ion takes the greatest, causing nickel less favoring by both nanosorbent types. This corresponds with the conception that ions which has small hydration radius is desirably selected and gathered at interface [2,24]. Furthermore, lead nitrate salt is less soluble in water in comparison with salts of nickel and cadmium. Therefore, lead ions had the highest adsorption rate. Moreover, elevated adsorption rate on the surface of Fe_3O_4 sorbent can be achieved depending on the highest molecular weight of the adsorbate, hence the sequence of the molecular weights for the used pollutant salts are: Pb $(NO_3)_2$ > Cd $(NO_3)_2$ > Ni

$(NO_3)_3.6H_2O$. The results in single system predicted that ability of commercial type to attract lead and nickel metals was competently higher than synthesized type to some extent. However, for cadmium ions, synthesized one was preferable opposed to commercial kind. As overall, concerning economy and cost of nanosorbent (imported from abroad) to obtain high percentage of contaminant removal from aqueous solution is similar to what has been resulted in this research. Therefore, synthesized Fe_3O_4 nanoparticles was dependable to be used in binary and tertiary systems due to its cheapness and availability of raw materials needed for its preparation in laboratory.

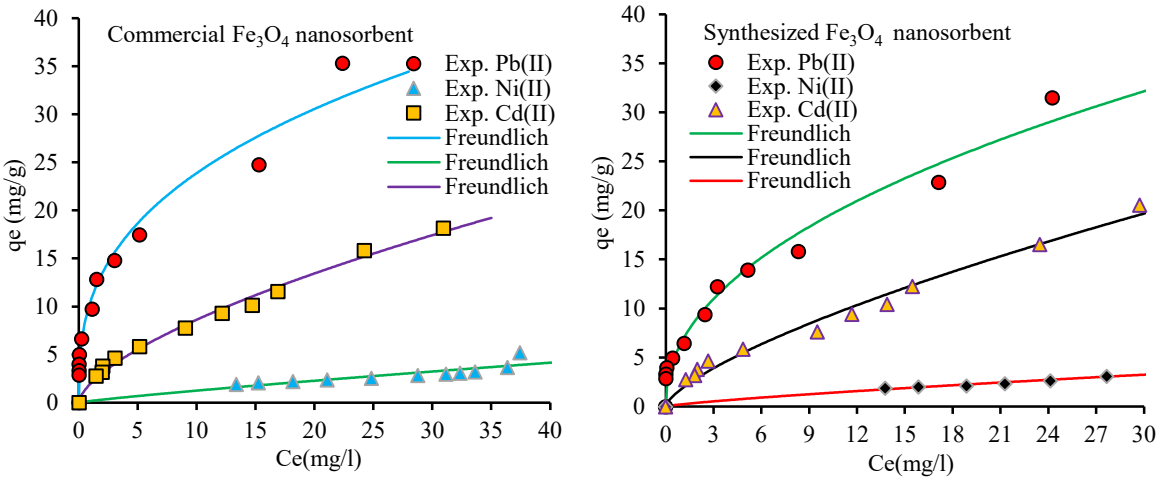

(a) (b)

Figure 5: Biosorption isotherms for lead, nickel, and cadmium ions onto

a) Commercial b) Synthesized Fe_3O_4 nanoparticles in single solute system .

Table 3: Parameters of single solute isotherm for Pb (II), Ni (II) and Cd (II) ions for commercial and synthesized Fe_3O_4 nanosorbent

Model	Parameter	Commercial Fe_3O_4			Synthesized Fe_3O_4		
		Pb (II)	Ni (II)	Cd (II)	Pb (II)	Ni (II)	Cd (II)
Langmuir $q_e = \frac{q_{max} b C_e}{(1+bC_e)}$	q_m(mg/g)	35.58	33.4	32.347	37.893	11.776	49
	b(l/mg)	0.27	0.0036	0.0372	0.12	0.0127	0.022
	R^2	0.8856	0.8496	0.9668	0.9204	0.9483	0.9601
Freundlich $q_e = KC_e^{1/n}$	K,	10.52	0.17	1.974	6.568	0.2178	1.8
	n	2.81	1.151	1.562	2.142	1.26	1.422
	R^2	0.9633	0.8542	0.9911	0.9696	0.9504	0.9838

4.5 *The effect of ions competition*

Figure 6 shows that the metal sorption uptake onto synthesized nanosorbent in binary and ternary systems was constrained by the presence of other metal ions. Results indicated that lead ions had more affinity compared to other metal ions. In binary system, uptake ability of the prepared form nanosorbent for lead ions downgraded by 7.7% and 30.8% with nickel and cadmium ions respectively, whereas this capability in ternary system dropped by 27.41%. Thus, during nanosorption, nickel creates less restriction to lead compared to cadmium ions. The most vital aspects that impact the relative selectivity of metal ions in solution are ionic radius and hydration energy [2]. From comparison of the three elements studied, the ionic radius order is Pb (II)> Cd (II)> Ni (II) and the hydration energy rates drop as the ionic radius grows up. Therefore, the selectivity sequence of favorable adsorption observed to be: Pb (II)> Cd (II)> Ni (II). This means that presence of nickel and cadmium in the aqueous solution had little impact on the nanosorption

of lead. Therefore, during the competition of ions to occupy the vacant sites, the adsorption capability of Cd(II) and Ni(II) are reduced [24]. Furthermore, lead nitrate salt is less soluble in water in comparison with nickel and cadmium salts. Therefore, elevated adsorption rate on the surface of Fe_3O_4 nanoparticles can be achievable depending on higher molecular weight of the adsorbate [39]. Hence, the sequence of the molecular weights for the used pollutant salts are: $Pb(NO_3)_2 > Cd(NO_3)_2 > Ni(NO_3)_3.6H_2O$. The gained data for binary and ternary element systems were well associated with interaction factor model giving the highest determinant coefficient. **Table 4** displays the parameters of each models.

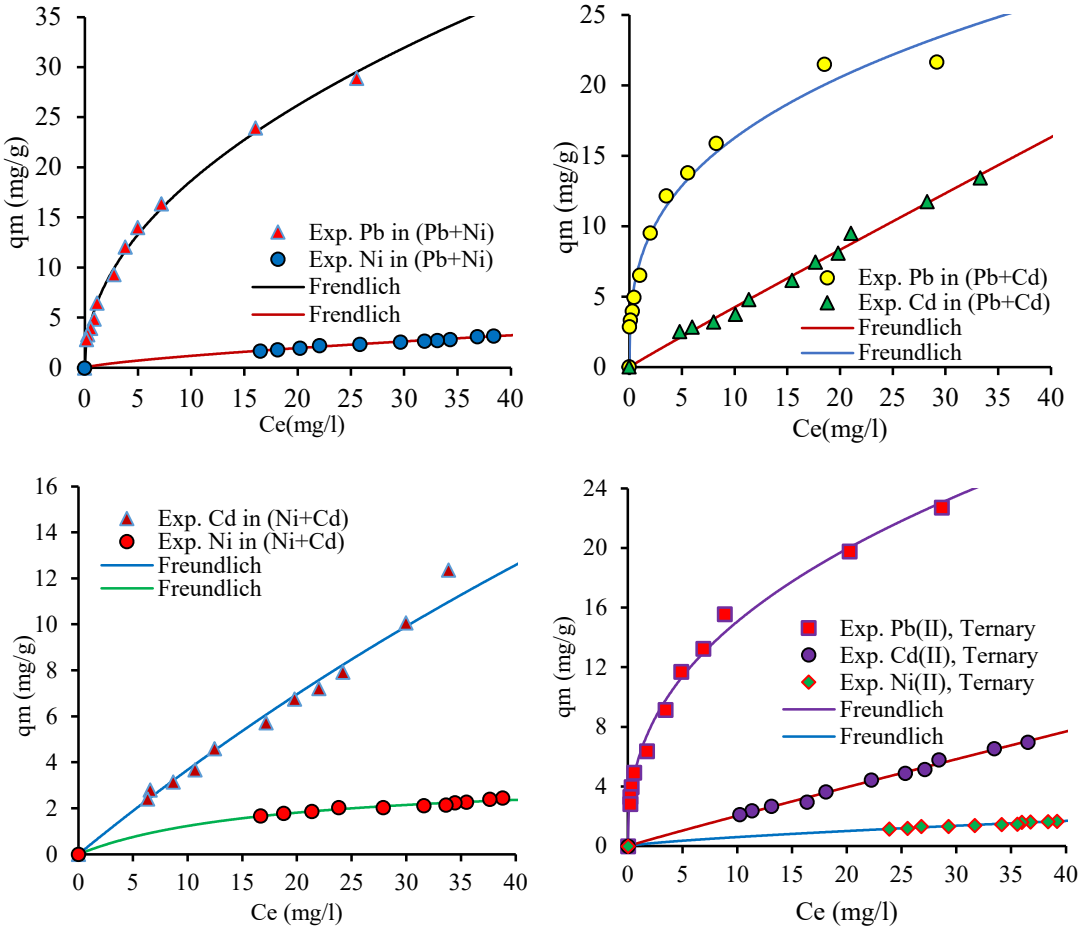

Figure 6: Isothermal adsorption for the three metal ions onto synthesized Fe_3O_4 nanoparticles in binary and ternary systems, $C_{o\ [pb,\ Ni,\ Cd]}$ =40mg/l, pH=6.

Table 4: Parameters of binary and ternary isotherm systems for lead, nickel and cadmium ions onto synthesized Fe_3O_4 nanoparticle.

Model	Parameters	Binary System					
		Pb and Ni		Pb and Cd		Ni and Cd	
		Pb	Ni	Pb	Cd	Ni	Cd
Extended Langmuir	q_m(mg/g)	35.82	8.578	23.06	74.158	3.41	65.04
	b(l/mg)	0.135	0.015	0.36	0.0064	0.057	0.006
	R^2	0.9803	09945	0.9537	0.9887	0.9914	0.9822
Interaction Factor	q_m(mg/g)	40.22	4.437	28.07	41.13	2.33	187.37
	η	49.48	0.225	78.21	4.84	0.225	3.43
	R^2	0.9923	0.9895	0.9794	0.9904	0.9886	0.9886

Ternary System				
Model	Parameters	Pb	Ni	Cd
Extended Langmuir	q_m(mg/g)	25.55	4.46	44.52
	b(l/mg)	0.185	0.015	0.005
	R^2	0.9562	0.9925	0.993
Interaction Factor	q_m(mg/g)	37.59	1.026	32.01
	η	74.19	0.15	1.04
	R^2	0.9854	0.9853	0.9592

4.6 *TEM image analysis*

The micrographs in **Figures 7 and 8** shows that up to 0.2 µm particle size was designated for both of iron oxide nanosorbents and irregular shape was notified from the photo scan images. The **Figures** also detected the nature of particles before and after adsorption of lead ions. The sticky nature of particles is notified due to agglomeration of metal pollutant on the nanoparticles. Both nanosorbents had a rough surface providing a large vacant area for metal ion interaction.

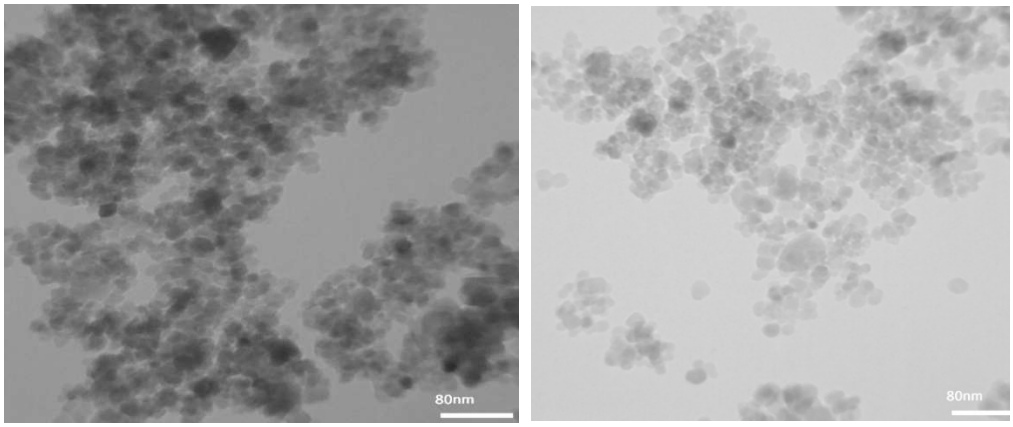

(a) (b)

Figure 7: Transmission electron micrographs of commercial Fe_3O_4 nonabsorbent.

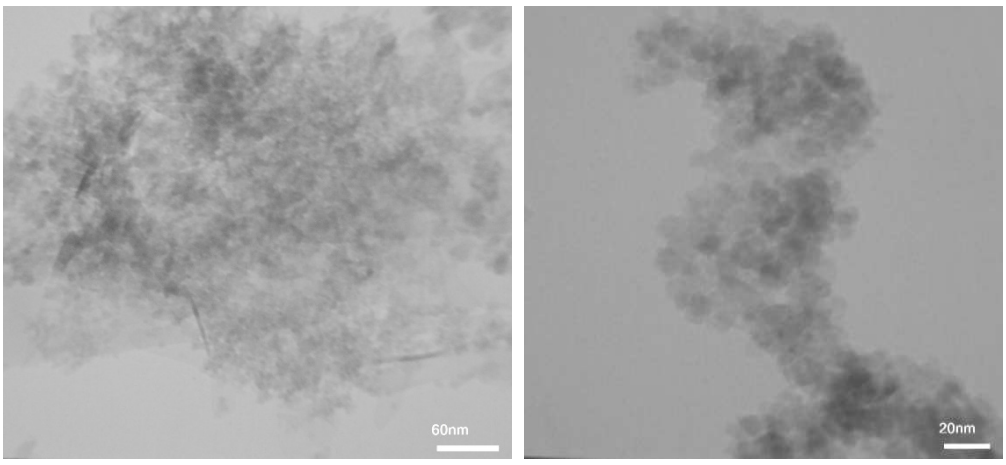

(a) (b)

Figure 8: Scanning electron micrographs of synthesized Fe_3O_4 nanosorbent.

.

4.7 *Fourier-Transform Infrared analysis*

Figure 9 demonstrated that several significant absorption peaks were participated in nanosorption of metal ions. The broad absorption peak in the region of 3421cm^{-1} band for commercial type is higher than peak 3394 cm^{-1} band for synthesized nanosorbent with only slight difference. The bands are correlated to −OH group. The typical peak around (578 and 442) cm^{-1} observed in spectra samples that are due to the stretching vibration mode related to metal–oxygen absorption band [16]. These brands associate with Fe−O bond, which also indicating that the nanosorbent in spectrum a is efficient than b. Moreover, peak perceived at (641 and 631) cm^{-1} for both sample types respectively belonged to aromatic group with few differences in their peaks. Finally, peaks notified at (1639 and 1638)cm^{-1} allocated to carboxyl groups, C=O bending vibration [20]. In this peak range, commercial sample nanosorbent is slightly more functional than synthesized sample in metal ion adsorption. FTIR graph in **Figure 9** indicates that hydroxyl, carboxyl amine and Fe−O groups are the main functional groups having responsibilities towards metal attraction to surface of both nanosorbents.

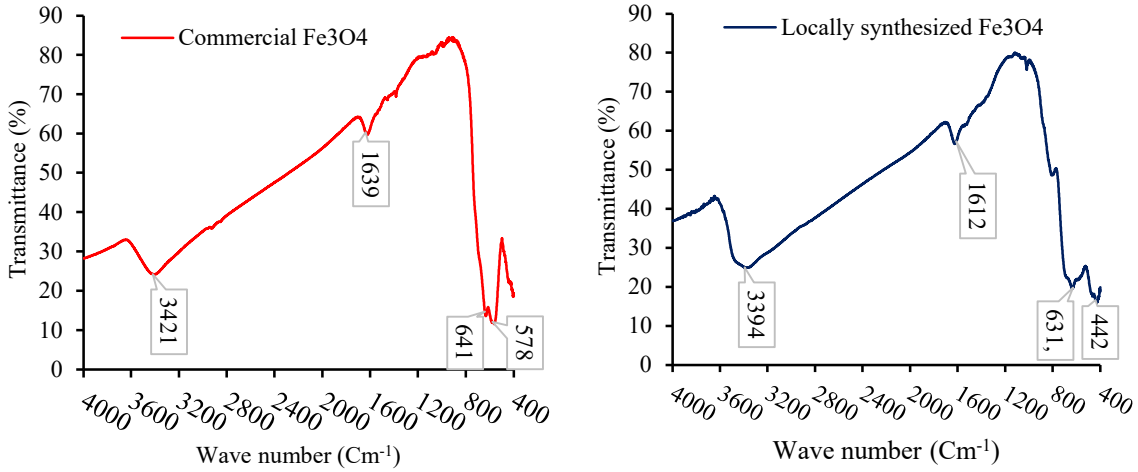

(a) (b)

Figure 9: FTIR spectra of raw Fe_3O_4 nanosorbent a) Commercial b) Synthesized.

4.8 *XRD (X-ray diffraction) analysis*

Figure 10 demonstrated that the diffraction prototype and two theta intensities for all peaks of commercial type are distinctively not corresponded to peaks observed in the synthesized. It also detected that the diffraction peaks in both of nanosorbents are low and broad due to small size effect and incomplete inner structure of the particle. The peak positions appearing at 2 thetas in commercial sample are 30.15°, 35.65°, 43.15°, 53.55, 57.15°, 62.85°, 74.65° attributing to diffractions from the planes of (220), (311), (400), (422), (511), (440) and (420) of magnetite Fe_3O_4 while for the synthesized sample, the peak positions are 26.75°, 30.15°, 35.15°, 39.25°, 46.55°, 56.15°, 62.95°, 67.85° belonging to diffractions from the planes of (130), (220), (311), (360), (400), (511), (440) of magnetite Fe_3O_4. The maximum intensity in the commercial type is (205) which is greater than what has been notified for synthesized one (197). This information confirmed that commercial form has more magnetite capability for adsorption opposed to the synthesized nanosorbent. Moreover, the graph revealed that the resulting magnetite Fe_3O_4 nanoparticles in both samples were mainly observed between (30-75) two theta (^{0}) x-ray deflection with big difference in the peaks located close to (30) two theta (^{0}) due to difference composition of Fe_3O_4 compound in the samples. Furthermore, analysis diffraction graphs discovered mainly some traits of massive magnetite compound phase, with intensive and high peaks signifying to magnetic nanoparticles [20].

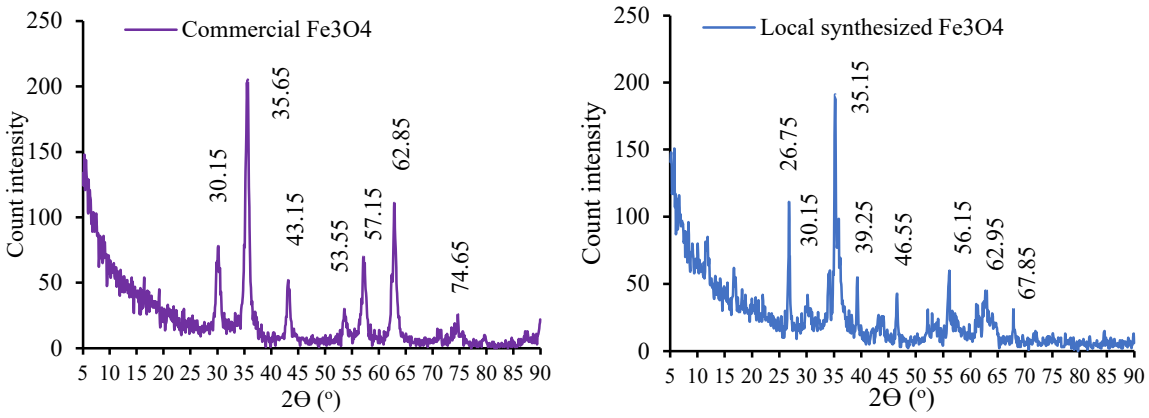

(a) (b)

Figure 10: XRD analysis for Fe3O4 nanoparticles a) Commercial b) Synthesized.

5. Conclusions

The adsorption of metal ions onto Fe_3O_4 nanoparticles is influenced by attractive forces between adsorbate cations of metal ions and negatively charged nanosorbent vacant sites. Several physiochemical properties of adsorbates in aqueous solution such as pH, solubility, surface charge, molecular weight, and size of adsorbate molecule, cooperate to play a fundamental role in the process mechanism. The transition of lead metal ions from the bulk liquid in the aqueous solution to the surface of both nanosorbents, faces low resistance compared to nickel and cadmium. Even though the viability and efficiency of the commercial type is distinctively greater than the synthesized type, the formulated Fe_3O_4 nanosorbent in the laboratory was preferred and chosen to demonstrate how the metal ion competition takes place in both binary and ternary systems. This is attributed to the fact that huge nanosorbent importation costs can be reduced and the synthesized Fe_3O_4 can replace the commercial category to remove contaminant ions from wastewater with significant and satisfactory efficiency.

Acknowledgments

The authors are thankful to the Kurdistan Institute for Strategic Studies and Scientific Research in Sulaimani, Iraq for their support and analytical test services. Also, Financial support from the University of Sulaimani was most helpful in achieving this work.

References

[1] Ahmed I., Iqbal H., Dhama K. (2017). Enzyme-based biodegradation of hazardous pollutants-An overview, J of experiment biol. and agric. sci. 5, 4, 402–411.

[2] Ahn Y., Choi, E., Kim E. (2003). Superparamagnetic relaxation in cobalt ferrite nanoparticles synthesized from hydroxide carbonate precursors, adv mater. sci. 5, 477–480.

[3] Alessa K., Khalili F. (2018). Heavy Metals Adsorption from Aqueous Solutions onto Unmodified and Modified Jordanian Kaolinite Clay: Batch and Column Techniques, Amer. J. appl. Chem. 6, 1, 25-34.

[4] Asgher M., Yasmeen O., Iqbal H. (2013). Enhanced decolorization of solar brilliant red 80 textile dye by an indigenous white rot fungus schizophyllum commune IBL-06, Saudi J of Biol. Sci. 20, 4, 347-52.

[5] Barrios-Estrada C., De Jesús Rostro-Alanis M., Muño P. (2018). Parra-Saldívar R, Emergent contaminants: Endocrine disruptors and their laccase-assisted degradation- A review, Sci Tota Envir. 612, 1516–1531.

[6] Bhuyan, M. S., Bakar, M. A., Akhtar, A., Hossain, M. B., Ali, M. M., & Islam, M. S. (2017). Heavy metal contamination in surface water and sediment of the Meghna River, Bangladesh. Environmental nanotechnology, monitor and manag. 8, 273-279.

[7] Chen Y., Zhao W., Wang H., Meng X., Zhang L. (2018). A novel polyamine-type starch/glycidyl methacrylate copolymer for adsorption of Pb(II), Cu(II), Cd(II) and Cr(III) ions from aqueous solutions, Roy soci open sci. 5, 180281.

[8] Cheng C., Wang J., Yang X., Li A., Philippe C. (2015). Adsorption of Ni (II) and Cd (II) from water by novel chelating sponge and the effect of alkali earth metal ions on the adsorption, J. Hazard Mater. 264, 332–341.

[9] Dipak P. (2017). Research on heavy metal pollution of river Ganga: A review, Anna of agrar sci. 15, 278-286.

[10] Ebrahim S., Sulaymon A., Alhares H. (2015). Competitive removal of Cu^{+2}, Cd^{+2}, Zn^{+2}, and Ni^{+2} ions onto iron oxide nanoparticles from wastewater, J. desal and water treat,, 1-15.

[11] Federation, W. E., & American Public Health Association. (2005). Standard methods for the examination of water and wastewater. American Public Health Association (APHA): Washington, DC, USA.

[12] Feng J., Mao J., Wen , X., Tu M. (2011). Ultrasonic-assisted in situ synthesis and characterization of superparamagnetic Fe3O4 nanoparticles, Alloys Compd. 509, 37, 9093–9097.

[13] Fu F., Wang Q. (2011). Removal of heavy metal ions from wastewaters: a review, J of Envir. Manag. 92(3), 407–418.

[14] Gupta, V. K., Nayak, A. (2012). Cadmium removal and recovery from aqueous solutions by novel adsorbents prepared from orange peel and Fe2O3 nanoparticles. Chemical Engineering Journal, 180, 81-90.

[15] Jaishankar M., Tseten T., Anbalagan N., Mathew B. (2014). Toxicity, mechanism and health effects of some heavy metals, Interdiscipl Toxico. 7, 2, 60–72.

[16] Ji S., Miao C., Liu H., Feng L., Yang X., Guo H. (2018). A Hydrothermal Synthesis of Fe_3O_4 @ C Hybrid Nanoparticle and Magnetic Adsorptive Performance to Remove Heavy Metal Ions in Aqueous Solution. Nanoscale research letters, 13, 1, 178.

[17] Kakaei A., Kazemeini M. (2016). Removal of Cd (II) in Water Samples Using Modified Magnetic Iron Oxide Nanoparticle, Iran J Toxicol. 10, 1.

[18] Kibria, G., Hossain , M., Mallick , D., Lau , T., & Wu , R. (2016). Monitoring of metal pollution in waterways across Bangladesh and ecological and public health implications of pollution, Chemosph, 165, 1–9.

[19] Kumar P., Ramalingam S., Kirupha, S., Murugesan P., Vidhadevi T., Sivanisan S. (2011). Adsorption behavior of nickel (II) onto cashew nut shell: Equilibrium, thermodynamics, kinetics, mechanism and process design, J of Chem Eng. 167, 1, 122–131.

[20] Lopez J. A., González F., Bonilla F. A., Zambrano G., Gómez M. E. (2010). Synthesis and characterization of Fe_3O_4 magnetic nanofluid, Revista Latinoamericana de Metalurgia Materiales, 60-66.

[21] Mahdavi S., Jalali M., Afkhami A. (2012). Removal of heavy metals from aqueous solutions using Fe_3O_4, ZnO, and CuO nanoparticles, J. of Nanopart Resea. 14, 846.

[22] Mahmoud A. M., Ibrahim F. A., Shaban S. A., Youssef N. A. (2015). Adsorption of heavy metal ion from aqueous solution by nickel oxide nano catalyst prepared by different methods. Egypt J. of Petrol. 24, 1, 27-35.

[23] Malik D. S., Jain C. K., Yadav A. K. (2017). Removal of heavy metals from emerging cellulosic low-cost adsorbents: a review. Applied water science, 7, 5, 2113-2136.

[24] Min J., Xiao S., Yingxin Z., Wenfang O., Yue W., Guanyi N. (2015). Effective adsorption of Cr (VI) on mesoporous Fe-functionalized Akadama clay: Optimization, selectivity, and mechanism, Appli Surace Sci. 344, 128-136.

[25] Mouni L., Belkhiri L., Bollinger J. C., Bouzaza A., Assadi A., Tirri, A., Remini, H. (2018). Removal of Methylene Blue from aqueous solutions by adsorption on Kaolin: Kinetic and equilibrium studies. Appl Cla Sci. 153, 38-45.

[26] Nassar N. (2010). Rapid removal and recovery of Pb(II) from wastewater by magnetic nanoadsorbents, J. Hazard Mater. 184, 538–546.

[27] Panneerselvam P., Morad N., Tan K. (2011). Magnetic nanoparticle (Fe_3O_4) impregnated onto tea waste for the removal of nickel (II) from aqueous solution, J. of Hazard Mater. 186, 160–168.

[28] Park, D., Yun Y., Park J. (2010). The past, present, and future trends of biosorption, Biotech and Biopro Eng. 15, 86–102.

[29] Parkinson G. (2016). Iron oxide surfaces, Surf Sci Repor, 71, 1, 272–365.

[30] Quintelas C., Fernandes B., Castro J., Figueiredo H. (2008). Biosorption of Cr(VI) by three different bacterial species supported on granular activated carbon—A comparative study, J. of Hazard Mater. 153, 799-809.

[31] Sandeep M., Kumar V. (2013). Magnetic nanoparticles-based biomedical and bioanalytical applications, Nanotechnol, 4.

[32] Singh, J., Upadhyay, S. K., Pathak, R. K., & Gupta, V. (2011). Accumulation of heavy metals in soil and paddy crop (Oryza sativa), irrigated with water of Ramgarh Lake, Gorakhpur, UP, India. Toxicol Envir Chem. 93, 3, 462-473.

[33] Soniya M., Krishnakumar G. (2015). Biosorption of Heavy Metals from Aqueous solution using

Mangrove fern Acrostichumaureum L, leaf Biomass as a Sorbent. Inter Resea Envir sci. 4, 11, 25−31.

[34] Tyagi I., Gupta V. K., Sadeg, H., Ghoshekandi R. S., & Makhlouf A. S. H. (2017). Nanoparticles as adsorbent; a positive approach for removal of noxious metal ions: a review. Sci Technol and Develop. 34, 3, 195-214.

[35] Ullah S., Zuberi A., Alagawany M., Farag M. R., Dadar M., Karthik K., Iqbal H. M. (2018). Cypermethrin induced toxicities in fish and adverse health outcomes: Its prevention and control measure adaptation, J. of envir manag. 206, 863-871.

[36] Vélez, E., Campillo, G. E., Morales, G., Hincapié, C., Osorio, J., Arnache, O., ... & Jaramillo, F. (2016). Mercury removal in wastewater by iron oxide nanoparticles. In Journal of Physics: Conference Series, 687, 1, 012050.

[37] Vijayaraghava K., Yun Y. (2008). Bacterial biosorbents and biosorption, Biotechnol Adv. 26, 266–291.

[38] Wang E., Guo Y., Yang L., Han M., Zhao J., Cheng X. (2010). Nanomaterials as sorbents to remove heavy metal ions in wastewater treatment, Envir Analyt Toxicol. 2, 2-7.

[39] Wasewar K., Kumar S., Prasad B. (2009). Adsorption of Tin using granular activated carbon, Envir Protect Sci. 3, 41-52.

[40] Wu W., Wu Z. (2015). Recent progress on magnetic iron oxide nanoparticles: synthesis, surface functional strategies and biomedical applications, Sci Technol Adv Mater. 16, 2.

[41] Xu Y., Chen Y. (2015). leaching heavy metals in municipal solid waste incinerator fly ash with chelator/biosurfactant mixed solution, Wast Manag and Resea. 33, 7, 652–661.

[42] Yogeshwari Y., Ragini G., Tenguriya, R. (2018). Management of Heavy Metal Pollution by using Bacterial Biomass, Inter J. Biotech Trends and Technol. 8, 1.

[43] Zhang S., Zhang X., Xiong Y., Wang G., Zheng N. (2015). Effective solidification/stabilisation of mercury-contaminated wastes using zeolites and chemically bonded phosphate ceramics, Wast Manag and Resea. 33, 2, 90-183.

مقارنة بين الجسيمات النانوية Fe_3O_4 التجارية والمصنعة محليا لإزالة الملوثات المعدنية الثقيلة في المياه العادمة

فاروق عبدالله رشيد الكردى[1]، شهلاء اسماعيل ابراهيم [2].

[1] جامعة السليمانية ،السليمانية، العراق، Farouk.rasheed@univsul.edu.iq

[2] جامعة بغداد ، بغداد، العراق، shahlaa.ebrahim@fulbrightmail.org

* الباحث الممثل: فاروق عبد الله رشيد الكردى Farouk.rasheed@univsul.edu.iq

نشر في: 31 آذار 2020

الخلاصة – اصبحت المياه العادمة الملوثة بالمعادن الثقيلة الضارة حاليًا قضية بيئية مهمة في جميع أنحاء العالم. في هذه الدراسة، كانت الجسيمات النانوية Fe_3O_4 التجارية والمصنعة محلياً استخدمت على إزالة أيونات الرصاص والنيكل والكادميوم في نظام عنصر واحد. تم اختبار الظروف التجريبية بما في ذلك الرقم الهيدروجيني، وزمن التجربة وتراكيز أيونات المعادن. كانت علاقة التوازن عند ثبوت درجة الحرارة لنظام مكون واحد مواتية والحد الأقصى من أيونات الرصاص والنيكل والكادميوم الممتزة على Fe_3O_4 التجاري كانت 35.3 ، 5.18 و 18.16 ملغم / غرام على التوالي في حين أن 31.5 و 4.36 و 20.56 ملغم / غرام على المحلي في أفضل درجة الحموضة 6 لمدة ساعة من التوازن وقت الاتصال. البيانات الأيزوثرم لكلا النوعين اشارت انهما يتطابقا بشكل جيد لموديل Freundlich. تُظهر التجارب أن أداء مادة النانو المُصنَّعة والتي تُعد مناسبة للاستخدام اقتصاديًا، تقترب من فعالية Fe_3O_4 التجاري. لذلك، تم اتخاذ شكل nanosorbent المحضر كمادة مازة عمليا واستخدامه في الأنظمة الثنائية والثلاثية لإظهار المنافسة بين الملوثات المعدنية. أشارت النتائج إلى أن أيونات الرصاص لها تقارب سريع ليتم امتزازها على الجسيمات النانوية في حين أن النيكل له جاذبية بطيئة. وأجريت أيضا فحوصات نقل الأشعة تحت الحمراء، حيود الأشعة السينية ، الأشعة السينية الضوئية ومسح الإلكترون المجهر لتحديد وإظهار خصائص لكلا من النوعين المواد النانوية.

الكلمات الرئيسية – أيون المعادن ، المادة النانوية ، الامتزاز ، المياه الملوثة.